Analysis of the efficiency with which geometrically asymmetric metal-vacuum-metal junctions can be used for the rectification of infrared and optical radiations

Mayer, Alexander; Chung, Moon; Lerner, Peter; Weiss, Brock; Miskovsky, Nicholas; Cutler, Paul

Published in:
Journal of vacuum science and technology. B, Nanotechnology & microelectronics

DOI:
10.1116/1.3698600

Publication date:
2012

Document Version
Early version, also known as pre-print

An analysis of the efficiency with which geometrically asymmetric metal-vacuum-metal junctions can be used for the rectification of infrared and optical radiations

A. Mayer†*, M.S. Chung‡, P.B. Lerner§, B.L. Weiss¶, N.M. Miskovsky♯ and P.H. Cutler♯

†*Laboratoire de Physique du Solide, University of Namur - FUNDP,*

Rue de Bruxelles 61, B-5000 Namur, Belgium

‡*Department of Physics, University of Ulsan, Ulsan 680-749, Korea*

§*Quantum Transistor, LLC, Ithaca, NY 14850, USA*

¶*Department of Physics, 130 CAC, The Pennsylvania*

State University, Altoona, PA 16601, USA and

♯ *Department of Physics, 104 Davey Laboratory,*

The Pennsylvania State University, University Park, PA 16802, USA

We simulate the rectification properties of geometrically asymmetric metal-vacuum-metal junctions in which one of the metals is flat while the other is extended by a sharp tip. We analyze in particular the efficiency with which the energy of incident radiations, with frequencies in the infrared through the visible, is transferred to the electrons that cross the junction. This time-dependent electronic scattering problem is solved by using a transfer-matrix methodology. In order to validate this technique, we first compare the results achieved using this quantum-mechanical scheme with those provided by models that are based on extrapolations of static current-voltage data. We then discuss concepts that are relevant to the efficiency with which energy is converted in these junctions. We finally analyze how this efficiency is affected by the amplitude and the angular frequency of the potentials that are induced in these junctions, the work function of the metallic contacts and the spacing between these contacts.

* Corresponding author ; Electronic address: alexandre.mayer@fundp.ac.be

I. INTRODUCTION

This work is the continuation of a series of articles in which we investigated the rectification properties of geometrically asymmetric metal-vacuum-metal junctions in which one of the metals is flat while the other is extended by a sharp tip.[1–5] This rectification consists in the fact that the application of oscillating potentials to these junctions will induce the circulation of currents with a strong dc component if we keep in conditions where the materials can respond to these oscillating potentials. Energy is transferred in this process from the source of these external potentials to the electrons that cross the junction. Geometrically asymmetric metal-vacuum-metal or metal-oxide-metal junctions have been proved useful for the rectification and the frequency-mixing of infrared radiations.[6–11] They also enabled the accurate measurement of infrared frequencies[12–14] and contributed to applications as fundamental as the measurement of the speed of light[15,16] and the determination of tunneling times.[17–19]

Geometrical, material and thermal asymmetries will all contribute to the rectification properties of these junctions.[1,2,17–21] In practice, the junction biasing will typically result from a laser beam whose energy is partially absorbed by a nanoantenna placed in series or integrated with the junction.[22–26] This biasing will be limited by the RC-time constant of the device.[17,27] The rectification achieved by the junction will depend in turn on the possibility for electrons to cross the junction before the induced electric field changes sign. This process is fundamentally limited by tunneling times, which are of the order of femtoseconds.[17–19,28,29] By carefully designing these junctions, it is actually possible to rectify optical frequencies as demonstrated by recent experimental work.[30–36] This makes these junctions useful for the development of high-speed electronics and for applications related to the harvesting of solar energy.[37,38]

Modeling the electromagnetic scattering processes that lead to the junction biasing would be situation-dependent and exceeds the scope of this work. We will rather focus on modeling the diode currents that result from this biasing. This modeling was achieved in previous work by using a transfer-matrix methodology.[1–5] We solve in this way the time-dependent electronic scattering problem exactly, by taking account of the three-dimensional aspects of the problem. It is interesting to compare the results achieved by using this quantum-mechanical scheme with those provided by a classical model in which it is merely assumed that the diode

current follows the instantaneous values of the external potential. This simplified picture provides a first approximation for the currents that cross the junction, which is expected to hold in the limit when the angular frequency Ω of the external potential goes to zero (approximation valid in infrared).[5] It also provides a convenient framework to analyze the results achieved by using a more exact quantum-mechanical scheme. In our previous work,[5] we used this classical model to study the impedance and the responsivity of geometrically asymmetric metal-vacuum-metal junctions. This study was essentially restricted to conditions where quasi-static approximations apply. This article will focus with more details on the efficiency with which energy is converted in these junctions when considering frequencies for which the usual classical approximations do not hold.

This article is organized according to the following lines. In Sec. II, we present the transfer-matrix methodology that is used for the quantum-mechanical simulations (this presentation includes important updates in the methodology). In Sec. III, we present different modeling techniques that are based on extrapolations of static current-voltage data. In Sec. IV, we compare the results provided by these different techniques for the mean diode current $< I >$ and for the mean energy $< P >$ gained per unit of time by the electrons that cross the junction. In Sec. V, we discuss different concepts that are relevant to the efficiency with which energy is converted in these junctions. We finally explore conditions that improve this efficiency. We investigate in particular how this efficiency is affected by the amplitude and the angular frequency of the external potential, the work function of the metallic contacts and the spacing between the cathode and the anode. The objective of this analysis is to provide useful insights for the realization of a practical device.

II. TIME-DEPENDENT MODELING OF ELECTRONIC SCATTERING USING A TRANSFER-MATRIX METHODOLOGY

We assume that the junction consists of two perfect metals separated by a vacuum gap of width D. The cathode in the region $z \leq 0$ and the anode in the region $z \geq D$ will be referred to as Region I and III, respectively. The intermediate region $0 \leq z \leq D$ will be referred to as Region II. The cathode supports a protrusion, which is part of Region II. The cathode and the anode are characterized by a Fermi energy E_{F} and a work function W. We will assume that a difference in electric potential $V(t) = V_{\mathrm{stat}} + V_{\mathrm{osc}} \cos(\Omega t)$ is established between the

two metallic contacts. We will adopt the convention that positive $V(t)$ corresponds to the emission of electrons from the cathode to the anode. We will define in this case the diode current $I(t)$ as positive.

We work in cylindrical coordinates and assume that the electrons are confined in a cylinder with radius R. We use the finite-difference techniques of Refs[39,40] to compute the potential energy $\hat{V}(\mathrm{r},t) = \hat{V}_{\mathrm{stat}}(\mathrm{r}) + \frac{1}{2}\left[\hat{V}_{\mathrm{osc}}(\mathbf{r},\Omega)e^{-i\Omega t} + \hat{V}_{\mathrm{osc}}(\mathbf{r},-\Omega)e^{i\Omega t}\right]$ in the three regions of our system.[3] We consider a Floquet expansion of the wave functions[41,42] and expand them as $\Psi(\mathbf{r},t) = \sum_{k=-N}^{N}\Psi_k(\mathbf{r})e^{-i(E+k\hbar\Omega)t/\hbar}$, where E refers to the electron energy. N is a cut-off parameter chosen sufficiently large to make final results independent of its particular value (for given values of V_{osc} and $\hbar\Omega$, N can be determined automatically by using the techniques of Ref.[2]). Introducing these expressions for $\hat{V}(\mathrm{r},t)$ and $\Psi(\mathbf{r},t)$ in the time-dependent Schrödinger equation $[-\frac{\hbar^2}{2m}\Delta + \hat{V}(\mathbf{r},t)]\Psi(\mathbf{r},t) = i\hbar\frac{\partial}{\partial t}\Psi(\mathbf{r},t)$, we find that the components $\Psi_k(\mathbf{r})$ of the wave functions follow an equation $[-\frac{\hbar^2}{2m}\Delta+\hat{V}_{\mathrm{stat}}(\mathbf{r})]\Psi_k(\mathbf{r})+\frac{1}{2}[\hat{V}_{\mathrm{osc}}(\mathbf{r},\Omega)\Psi_{k-1}(\mathbf{r})+\hat{V}_{\mathrm{osc}}(\mathbf{r},-\Omega)\Psi_{k+1}(\mathbf{r})] = (E+k\hbar\Omega)\Psi_k(\mathbf{r})$ in which the oscillating part of the potential energy turns out to be responsible for the coupling between the different components $\Psi_k(\mathbf{r})$ of the wave functions. This coupling can be interpreted as the absorption or emission of energy quanta $\hbar\Omega$ by the electrons that cross the junction.

Solving the time-dependent Schrödinger equation in Region I, the boundary states in this region turn out to be given by

$$\Psi^{\mathrm{I},\pm}_{m,j,k}(\rho,\phi,z,t) = \frac{RJ_m(k_{m,j}\rho)\exp(im\phi)}{\sqrt{2\int_0^R \rho J_m^2(k_{m,j}\rho)d\rho}}e^{\pm i\sqrt{(2m/\hbar^2)(E+k\hbar\Omega-\hat{V}_{\mathrm{I}})-k_{m,j}^2}z}e^{-i(E+k\hbar\Omega)t/\hbar}, \qquad (1)$$

where J_m refers to the Bessel functions and the $\pm$ signs to the propagation direction.[2] m is an angular momentum quantum number and j an enumeration parameter for the lateral wavevectors $k_{m,j}$, which are solutions of $J_m'(k_{m,j}R) = 0$.[43,44] $\hat{V}_{\mathrm{I}} = eV_{\mathrm{stat}} - W - E_{\mathrm{F}}$ finally refers to the constant potential energy in Region I (e refers to the elementary positive charge).

The boundary states in Region III are given by

$$\Psi^{\mathrm{III},\pm}_{m,j,k}(\rho,\phi,z,t) = \frac{RJ_m(k_{m,j}\rho)\exp(im\phi)}{\sqrt{2\int_0^R \rho J_m^2(k_{m,j}\rho)d\rho}}e^{\pm i\sqrt{(2m/\hbar^2)(E+\lambda_k-\hat{V}_{\mathrm{III}})-k_{m,j}^2}z}\sum_{k'=-N}^{N}V_{k',k}e^{-i(E+k'\hbar\Omega)t/\hbar} \qquad (2)$$

where $\hat{V}_{\mathrm{III}} = -W - E_{\mathrm{F}}$ refers to the constant part of the potential energy in Region III.[2] The complete expression for the potential energy in Region III is actually $\hat{V}_{\mathrm{III}}(t) = \hat{V}_{\mathrm{III}} - eV_{\mathrm{osc}}\cos(\Omega t)$, which also accounts for the contribution due to the oscillating potential. λ_k

and $V_{k',k}$ refer to the eigenvalues and the k'-components of the corresponding eigenvectors of a matrix M, whose elements are defined by $M_{k',k} = k\hbar\Omega\delta_{k',k} + \frac{eV_{\rm osc}}{2}(\delta_{k',k+1} + \delta_{k',k-1})$.

The boundary states $\Psi^{\rm I,\pm}_{m,j,k}$ and $\Psi^{\rm III,\pm}_{m,j,k}$ are associated with a mean energy $E + k\hbar\Omega$.[2] This representation hence accounts for the absorption or emission of energy quanta $\hbar\Omega$ by the electrons that cross the junction. By using the techniques of Refs[2,3], one can then establish scattering solutions of the form

$$\Psi^{+}_{m,j,0} \overset{z\leqq 0}{\equiv} \Psi^{\rm I,+}_{m,j,0} + \sum_{m',j',k'} S^{-+}_{(m',j',k'),(m,j,0)} \Psi^{\rm I,-}_{m',j',k'} \overset{z\geqq D}{\equiv} \sum_{m',j',k'} S^{++}_{(m',j',k'),(m,j,0)} \Psi^{\rm III,+}_{m',j',k'}, \quad (3)$$

$$\Psi^{-}_{m,j,0} \overset{z\leqq 0}{\equiv} \sum_{m',j',k'} S^{--}_{(m',j',k'),(m,j,0)} \Psi^{\rm I,-}_{m',j',k'} \overset{z\geqq D}{\equiv} \Psi^{\rm III,-}_{m,j,0} + \sum_{m',j',k'} S^{+-}_{(m',j',k'),(m,j,0)} \Psi^{\rm III,+}_{m',j',k'}, \quad (4)$$

which correspond to single incident states $\Psi^{\rm I,+}_{m,j,0}$ and $\Psi^{\rm III,-}_{m,j,0}$ in Region I and III respectively. The transfer matrices $\mathbf{S}^{++}$ and $\mathbf{S}^{--}$ contain the coefficients of the transmitted states, while the transfer matrices $\mathbf{S}^{-+}$ and $\mathbf{S}^{+-}$ contain the coefficients of the reflected states. These solutions are obtained by taking account of the three-dimensional aspects of the problem. The time-dependence of the external potential is here treated exactly. In contrast, the techniques presented in Sec. III will rely on extrapolations of data achieved with static potentials.

Considering the contribution of every incident state in Region I and III, the mean diode current is finally given by

$$\begin{aligned} < I_{\rm TM} > \; = \; & \frac{2e}{h} \int_{\hat{V}_{\rm I}}^{+\infty} f_{\rm I}(E) \sum_{m,j} \sum_{k',m',j'} \frac{\sqrt{\frac{2m}{\hbar^2}(E + \lambda_{k'} - \hat{V}_{\rm III}) - k^2_{m',j'}}}{\sqrt{\frac{2m}{\hbar^2}(E - \hat{V}_{\rm I}) - k^2_{m,j}}} |S^{++}_{(m',j',k'),(m,j,0)}|^2 dE \\ - \; & \frac{2e}{h} \int_{\hat{V}_{\rm III}}^{+\infty} f_{\rm III}(E) \sum_{m,j} \sum_{k',m',j'} \frac{\sqrt{\frac{2m}{\hbar^2}(E + k'\hbar\Omega - \hat{V}_{\rm I}) - k^2_{m',j'}}}{\sqrt{\frac{2m}{\hbar^2}(E - \hat{V}_{\rm III}) - k^2_{m,j}}} |S^{--}_{(m',j',k'),(m,j,0)}|^2 dE \quad (5) \end{aligned}$$

where the different summations are restricted to propagative states (the derivation of this expression can be found in Appendix A). The Fermi factors $f_{\rm I}(E) = 1/\{1 + \exp[(E - \mu_{\rm I})/(k_{\rm B}T)]\}$ and $f_{\rm III}(E) = 1/\{1 + \exp[(E - \mu_{\rm III})/(k_{\rm B}T)]\}$, with $\mu_{\rm I} = eV_{\rm stat} - W$, $\mu_{\rm III} = -W$, $k_{\rm B}$ the constant of Boltzmann and T the temperature, account for the filling of the electronic states in Region I and III. It is through these factors that the temperature T of the device can be taken into account.

There are different possibilities to determine the mean energy gained per unit of time by the electrons that cross the junction (we implicitly understand this energy as gained from the source of the external potential). In the context of this quantum mechanical scheme,

we have to compare the kinetic energy of the transmitted states with that of the incident states. Differences in the kinetic energy will be due either to the static part of the electric potential ($V_{\rm stat}$) or to the absorption/emission of energy quanta $\hbar\Omega$ by the electrons that cross the junction. Considering these two contributions, the mean energy gained per unit of time by the electrons that cross the junction will be given by

$$\begin{aligned} < P_{\rm TM} > \; &= V_{\rm stat} < I_{\rm TM} > \\ &+ \frac{2e}{h}\int_{\hat{V}_{\rm I}}^{+\infty} f_{\rm I}(E)\sum_{m,j}\sum_{k',m',j'}\frac{k'\hbar\Omega}{e}\frac{\sqrt{\frac{2m}{\hbar^2}(E+\lambda_{k'}-\hat{V}_{\rm III})-k_{m',j'}^2}}{\sqrt{\frac{2m}{\hbar^2}(E-\hat{V}_{\rm I})-k_{m,j}^2}}|S^{++}_{(m',j',k'),(m,j,0)}|^2 dE \\ &+ \frac{2e}{h}\int_{\hat{V}_{\rm III}}^{+\infty} f_{\rm III}(E)\sum_{m,j}\sum_{k',m',j'}\frac{k'\hbar\Omega}{e}\frac{\sqrt{\frac{2m}{\hbar^2}(E+k'\hbar\Omega-\hat{V}_{\rm I})-k_{m',j'}^2}}{\sqrt{\frac{2m}{\hbar^2}(E-\hat{V}_{\rm III})-k_{m,j}^2}}|S^{--}_{(m',j',k'),(m,j,0)}|^2 dE \end{aligned} \quad (5)$$

This relation is demonstrated with details in Appendix A.

A second way to evaluate the mean energy gained per unit of time by the electrons that cross the junction is to compute the work achieved per unit of time by the electric field on the electrons that cross the junction. In the context of this quantum-mechanical scheme, one can only get an approximation for this quantity, which is given by

$$< P_{\rm TM-CL} >= \frac{\Omega}{2\pi}\int_0^{2\pi/\Omega} V(t) I_{\rm TM}(t) dt, \quad (7)$$

where $I_{\rm TM}(t)$ refers to the current provided by the transfer-matrix technique.[2] This formula is an approximation because it assumes implicitly that the variations of the external potential $V(t) = V_{\rm stat} + V_{\rm osc}\cos(\Omega t)$ are negligible during the time taken by electrons to cross the junction. It provides however a useful verification of Eq. 6 in the limit when $\Omega \to 0$. Given the Fourier decomposition $I_{\rm TM}(t) = \sum_{k=-2N}^{2N} I_k e^{ik\Omega t}$ of the diode current, $< P_{\rm TM-CL} >$ is actually given by $< P_{\rm TM-CL} >= V_{\rm stat} I_0 + V_{\rm osc}{\rm Re}[I_1]$.[2]

Eq. 5 for the mean diode current $< I >$ and Eq. 6 for the mean energy $< P >$ gained per unit of time by the electrons that cross the junction actually replace the expressions (9), (10), (14) and (15) given in Ref.[2] for the calculation of these quantities. In this previous work, we included in $< I >$ and $< P >$ factors of the form $[1 - f_{\rm III}(E)]$ and $[1 - f_{\rm I}(E)]$ to account for the availability of free states in the regions in which electrons are transmitted. Although the inclusion of these factors is legitimate with static potentials, they should not appear when considering oscillating potentials. This point is demonstrated in Appendix B.

III. MODELING TECHNIQUES BASED ON EXTRAPOLATIONS OF STATIC CURRENT-VOLTAGE DATA

We present here three alternative methods to evaluate the mean diode current $< I >$ and the mean energy $< P >$ gained per unit of time by the electrons that cross the junction. In contrast with the technique given in Sec. II, these methods essentially consist of an extrapolation of static current-voltage data.

A. Classical expressions for $< I >$ and $< P >$

Let us assume that the *static* $I_{\rm stat}(V_{\rm stat})$ characteristics of the junction are known. For the applications considered here-after, these $I_{\rm stat}(V_{\rm stat})$ data will be established by using the transfer-matrix technique with an external potential given by $V(t) = V_{\rm stat}$, where $V_{\rm stat}$ will range between -15 V and 15 V. We want to evaluate from these static data the diode current $I(t)$ that results from an external potential of the form $V(t) = V_{\rm stat} + V_{\rm osc}\cos(\Omega t)$.

In this classical approach, it is merely assumed that the diode current follows the instantaneous values of the external potential. The diode current $I(t)$ is then given by $I(t) = I_{\rm stat}[V_{\rm stat} + V_{\rm osc}\cos(\Omega t)]$, which we expand as $I(t) = \sum_{n=0}^{\infty} \frac{1}{n!}\frac{d^n I_{\rm stat}}{dV_{\rm stat}^n}[V(t) - V_{\rm stat}]^n = \left(I_{\rm stat} + \frac{V_{\rm osc}^2}{4}\frac{d^2 I_{\rm stat}}{dV_{\rm stat}^2}\right) + V_{\rm osc}\frac{dI_{\rm stat}}{dV_{\rm stat}}\cos(\Omega t) + \frac{V_{\rm osc}^2}{4}\frac{d^2 I_{\rm stat}}{dV_{\rm stat}^2}\cos(2\Omega t)$ if we keep to second order in $V_{\rm osc}$ ($I_{\rm stat}$, $\frac{dI_{\rm stat}}{dV_{\rm stat}}$ and $\frac{d^2 I_{\rm stat}}{dV_{\rm stat}^2}$ are calculated at the external potential $V_{\rm stat}$).[5,27,34,45,46]

The mean diode current is hence given within this approach by

$$< I_{\rm CL} >= \frac{\Omega}{2\pi}\int_0^{2\pi/\Omega} I(t)dt = I_{\rm stat} + \frac{V_{\rm osc}^2}{4}\frac{d^2 I_{\rm stat}}{dV_{\rm stat}^2} \tag{8}$$

while the energy gained per unit of time by the electrons that cross the junction will be given by

$$< P_{\rm CL} >= \frac{\Omega}{2\pi}\int_0^{2\pi/\Omega} V(t)I(t)dt = V_{\rm stat} < I_{\rm CL} > + \frac{V_{\rm osc}^2}{2}\frac{dI_{\rm stat}}{dV_{\rm stat}}. \tag{9}$$

These results are implicitly based on the assumption that the time taken by the electrons to cross the junction is negligible compared to the period $2\pi/\Omega$ of the oscillating part of the external potential. This assumption is valid in the limit when $\Omega \to 0$ (infrared). When considering optical frequencies, this assumption is however not valid and significant differences between classical and quantum-mechanical approaches will indeed appear.

B. Finite-difference expressions for $< I >$ and $< P >$

The expressions 8 and 9 for the mean diode current $< I >$ and for the mean energy $< P >$ gained per unit of time by the electrons that cross the junction do not account for the photon energy $\hbar\Omega$. As demonstrated in Sec. IV, significant differences with the time-dependent transfer-matrix results appear for photon energies of the order of the electronvolt. One can get closer to these quantum-mechanical results by considering finite-difference expressions for the calculation of $< I >$ and $< P >$.

The finite-difference formulation of the classical expression $< I_{\rm CL} >= I_{\rm stat} + \frac{V_{\rm osc}^2}{4}\frac{d^2 I_{\rm stat}}{dV_{\rm stat}^2}$ is given by

$$< I_{\rm FD} >= I_{\rm stat} + \frac{V_{\rm osc}^2}{4}\frac{I_{\rm stat}(V_{\rm stat}+\frac{\hbar\Omega}{e}) - 2I_{\rm stat}(V_{\rm stat}) + I_{\rm stat}(V_{\rm stat}-\frac{\hbar\Omega}{e})}{(\frac{\hbar\Omega}{e})^2}, \tag{10}$$

where the discretization step used for the evaluation of $\frac{d^2 I_{\rm stat}}{dV_{\rm stat}^2}$ actually corresponds to the photon energy $\hbar\Omega$.[34,45,46] This makes sense from a physical point of view since electrons absorb or emit *entire photons* (in contrast with infinitely small fractions of these photons).

The finite-difference formulation of the classical expression $< P_{\rm CL} >= V_{\rm stat} < I_{\rm CL} > + \frac{V_{\rm osc}^2}{2}\frac{dI_{\rm stat}}{dV_{\rm stat}}$ is then given by

$$< P_{\rm FD} >= V_{\rm stat} < I_{\rm FD} > + \frac{V_{\rm osc}^2}{2}\frac{I_{\rm stat}(V_{\rm stat}+\frac{\hbar\Omega}{e}) - I_{\rm stat}(V_{\rm stat}-\frac{\hbar\Omega}{e})}{2(\frac{\hbar\Omega}{e})}, \tag{11}$$

where $\frac{dI_{\rm stat}}{dV_{\rm stat}}$ is also evaluated by using a discretization step that corresponds to the photon energy.[45]

In contrast with the classical expressions 8 and 9, $< I_{\rm FD} >$ and $< P_{\rm FD} >$ do account for the photon energy $\hbar\Omega$. We will see in Sec. IV that $< I_{\rm FD} >$ and $< P_{\rm FD} >$ provide a reasonable approximation of the time-dependent transfer-matrix results for photon energies $\hbar\Omega$ not exceeding 1 eV in the conditions of this work.

C. Tien-Gordon expressions for $< I >$ and $< P >$

The finite-difference expression $< I_{\rm FD} >$ turns out to be a special limiting case of the Tien-Gordon expression[45–47]

$$< I_{\rm TG} >= \sum_{n=-\infty}^{+\infty} J_n^2(\alpha) I_{\rm stat}(V_{\rm stat} + n.\frac{\hbar\Omega}{e}), \tag{12}$$

in which $\alpha = \frac{eV_{\rm osc}}{\hbar\Omega}$. This formula reduces indeed to the finite-difference expression, Eq. 10, when $\alpha \ll 1$ (i.e., in the case of a small oscillating-voltage amplitude $V_{\rm osc}$ or a large photon energy $\hbar\Omega$).

The energy gained per unit of time by the electrons that cross the junction is given within this approximation by

$$< P_{\rm TG} >= \sum_{n=-\infty}^{+\infty} n\frac{\hbar\Omega}{e} J_n^2(\alpha) I_{\rm stat}(V_{\rm stat} + n.\frac{\hbar\Omega}{e}), \tag{13}$$

which also reduces to the finite-difference expression, Eq. 11, when $\alpha \ll 1$.[45,47]

These expressions are established for conditions that require a small oscillating-voltage amplitude $V_{\rm osc}$ (it is assumed indeed that the transmission probabilities do not change significantly on the energy scale given by $eV_{\rm osc}$).[45,47] They constitute however a more exact treatment, compared to the finite-difference expressions 10 and 11.

IV. COMPARISON BETWEEN THE DIFFERENT MODELS

For the comparison between the different models, we consider a metal-vacuum-metal junction with a hemispherical protrusion of 1 nm. The gap spacing D between the cathode and the anode is 2 nm (the distance between the apex of the protrusion and the anode is 1 nm).[48] The radius R considered for the application of the transfer-matrix technique is 3 nm. We assume that the two metallic contacts consist of tungsten ($E_{\rm F}$=19.1 eV and W=4.5 eV). We take a room temperature T of 300 K.

We assume that this junction is subject to an external potential $V(t) = V_{\rm stat} + V_{\rm osc}\cos(\Omega t)$, where $V_{\rm stat}$=0 V and $V_{\rm osc}$=0.1 V. We will consider angular frequencies Ω that correspond to energy quanta $\hbar\Omega$ between 0.1 and 5 eV. The static and oscillating components of the potential energy $\hat{V}(\mathbf{r}, t)$ that is used with the time-dependent transfer-matrix technique are represented in Fig. 1.

The mean diode current $< I >$ achieved when considering energy quanta $\hbar\Omega$ between 0.1 and 5 eV are represented in Fig. 2. This figure actually compares: (i) the mean diode current $< I_{\rm CL} >$ provided by the classical expression (Eq. 8), (ii) the mean diode current $< I_{\rm FD} >$ provided by the finite-difference expression (Eq. 10), (iii) the mean diode current $< I_{\rm TG} >$ provided by the Tien-Gordon expression (Eq. 12), and finally (iv) the mean diode current $< I_{\rm TM} >$ provided by the time-dependent transfer-matrix technique (Eq. 5). The

representation also includes the result achieved when using the transfer-matrix technique of Ref.[2].

The different models provide similar results in the limit when $\hbar\Omega \rightarrow 0$. The classical expression $< I_{\rm CL} >$ does not account for the photon energy $\hbar\Omega$ as mentioned previously. The finite-difference expression $< I_{\rm FD} >$ and the Tien-Gordon expression $< I_{\rm TG} >$ do account for this photon energy. They provide quasi-identical results (this is due to the fact the parameter $\alpha = \frac{eV_{\rm osc}}{\hbar\Omega}$ is always smaller than 1 for the values of $V_{\rm osc}$ and $\hbar\Omega$ considered). The time-dependent transfer-matrix result keeps close to the finite-difference and the Tien-Gordon expressions when considering $\hbar\Omega$ values below 2 eV. For higher photon energies, the mean diode current turns out to be significantly higher than the results predicted by $< I_{\rm FD} >$ or $< I_{\rm TG} >$. The transfer-matrix methodology accounts indeed for the absorption of energy quanta $\hbar\Omega$ by the electrons that cross the junction. For photon energies higher than 2 eV, this increases significantly their probability to cross the junction and higher diode currents are obtained. We note that the currents provided by the time-dependent transfer-matrix technique of Sec. II are different from those obtained when using the techniques of Ref.[2]. This discrepancy is especially pronounced with small values of $V_{\rm osc}$ since factors of the form $[1 - f_{\rm III}(E)]$ and $[1 - f_{\rm I}(E)]$ have in this case a significant impact (results corresponding to values of $V_{\rm osc}$ of the order of 1 V or higher tend to be identical).

The mean energy $< P >$ gained per unit of time by the electrons that cross the junction is represented in Fig. 3. The figure compares: (i) the result $< P_{\rm CL} >$ provided by the classical expression (Eq. 9), (ii) the result $< P_{\rm FD} >$ provided by the finite-difference expression (Eq. 11), (iii) the result $< P_{\rm TG} >$ provided by the Tien-Gordon expression (Eq. 13), and (iv) the result $< P_{\rm TM} >$ provided by the time-dependent transfer-matrix technique (Eq. 6). The representation includes for comparison the result obtained when using the transfer-matrix technique of Ref.[2] and the result $< P_{\rm TM-CL} >$ provided by a classical integration of the transfer-matrix currents (Eq. 7).

These different models agree again in the limit when $\hbar\Omega \rightarrow 0$, except for the result achieved when using the transfer-matrix technique of Ref.[2] (factors of the form $[1 - f_{\rm III}(E)]$ and $[1 - f_{\rm I}(E)]$ are responsible in this case for a significant reduction of the calculated values). The time-dependent transfer-matrix technique of Sec. II does provide a result that agrees with $< P_{\rm CL} >$, $< P_{\rm FD} >$ and $< P_{\rm TG} >$ in the limit when $\hbar\Omega \rightarrow 0$. This validates the modifications introduced in this methodology. The classical expression $< P_{\rm CL} >$ provides

again a result that is independent of the photon energy $\hbar\Omega$. The finite-difference expression $< P_{\rm FD} >$ and the Tien-Gordon expression $< P_{\rm TG} >$ provide quasi-identical results. $< P_{\rm FD} >$ and $< P_{\rm TG} >$ both account for the photon energy. The time-dependent transfer-matrix technique provides results that are significantly higher than $< P_{\rm FD} >$ and $< P_{\rm TG} >$ when the photon energy $\hbar\Omega$ exceeds 2 eV. This is due again to the absorption of energy quanta $\hbar\Omega$ by the electrons that cross the junction (this absorption increases significantly their probability to cross the junction). The results $< P_{\rm TM-CL} >= \frac{\Omega}{2\pi}\int_0^{2\pi/\Omega} V(t) I_{\rm TM}(t) dt$ achieved when integrating classically the transfer-matrix currents are consistent with those discussed so far as long as the time required by electrons to cross the junction keeps negligible compared to the period $2\pi/\Omega$ of the external potential. This stops being the case for a photon energy $\hbar\Omega$ of the order of 3.3 eV, which corresponds to a traversal time of 1.2×10^{-15} sec. This value is consistent with earlier estimations of these traversal times.[18,19,29]

V. QUANTUM EFFICIENCY AND ENERGY CONVERSION EFFICIENCY

We can now analyze the efficiency with which energy is converted in these junctions. This efficiency can be characterized by the *quantum efficiency*, which is given by

$$\eta = \frac{[< I > - I_{\rm stat}]/[< P > - V_{\rm stat} I_{\rm stat}]}{e/\hbar\Omega} \tag{14}$$

if we substract from $< I >$ and $< P >$ the contributions $I_{\rm stat}$ and $V_{\rm stat} I_{\rm stat}$ obtained when $V_{\rm osc}$=0 V. The quantities $[< I > - I_{\rm stat}]$ and $[< P > - V_{\rm stat} I_{\rm stat}]$ used for this definition only account for the effects of the oscillating field (it is the energy of this oscillating field that the junction aims at converting). The quantum efficiency η is related to the classical responsivity $S = (d^2 I_{\rm stat}/dV_{\rm stat}^2)/(dI_{\rm stat}/dV_{\rm stat})$ of the junction by $\eta = \frac{1}{2}\frac{\hbar\Omega}{e} S$ in conditions where the classical formalism of Sec. III A applies.[5,27,33] The results achieved by using the different models for the calculation of $< I >$ and $< P >$ are represented in Fig. 4. These results correspond to a static potential $V_{\rm stat}$ of 0 V and to an oscillating-voltage amplitude $V_{\rm osc}$ of 0.1 V. The different models are in close agreement for photon energies $\hbar\Omega$ smaller than 2 eV. The time-dependent transfer-matrix results indicate a maximal quantum efficiency η of 42.5% for $\hbar\Omega$=3.6 eV.

The quantum efficiency η as defined by Eq. 14 relates quantities that are associated with the electrons that cross the junction. For practical applications, it is useful to relate the

power that could be delivered to an external load with the mean energy required per unit of time to establish the oscillating field in the junction. The mean energy $< P >$ gained per unit of time by the electrons that cross the junction is actually associated with currents whose oscillations are too fast to be used by any conventional device when optical frequencies are considered. A definition of power that meets the idea that rectification is the key process to deliver energy to an external load is given by $< P_{\rm out,dc} >= (V_{\rm stat} + V_{\rm rect}) \times < I >$ in which we consider only the dc components of the voltage and of the diode current. The *rectified potential* $V_{\rm rect}$ corresponds to the effective static bias that would provide the same rectified diode current ($< I > -I_{\rm stat}$) as that associated with the oscillating field. The rectified potential $V_{\rm rect}$ can be evaluated in a first-order approximation from the relation $V_{\rm rect} \times \frac{dI_{\rm stat}}{dV_{\rm stat}} =< I > -I_{\rm stat}$. In situations where $V_{\rm stat}$=0 V, the output dc power is simply given by $< P_{\rm out,dc} >=< I >^2 /(dI_{\rm stat}/dV_{\rm stat})$. It corresponds to the power that could be delivered to an external load. The mean energy required per unit of time to establish the oscillating field in the junction is given by $< P_{\rm in,osc} >= \frac{1}{2}\frac{\Omega}{2\pi}\frac{CV_{\rm osc}^2}{2}$, where C represents the capacitance of the junction (once the oscillating field $\mathbf{E}_{\rm osc}(\mathbf{r})$ has been calculated for each point $\mathbf{r}$ in the junction,[39] the capacitance C is calculated from the relation $C = \frac{\epsilon_0 \iiint \epsilon(\mathbf{r})|\mathbf{E}_{\rm osc}(\mathbf{r})|^2 dV}{V_{\rm osc}^2}$ in which the integration is performed over the whole Region II). The *energy conversion efficiency* that is relevant to the oscillating part of the external potential is finally given by

$$\eta_{\rm ECE} = \frac{[< P_{\rm out,dc} > -V_{\rm stat} I_{\rm stat}]}{< P_{\rm in,osc} >}, \tag{15}$$

where we substract from $< P_{\rm out,dc} >$ the value achieved when $V_{\rm osc}$= 0 V.

We represented in Fig. 5 the results achieved for $\eta_{\rm ECE}$ when using the different models of Sec. II and III for the calculation of $< I >$. These results correspond to a static potential $V_{\rm stat}$ of 0 V and to an oscillating-voltage amplitude $V_{\rm osc}$ of 0.1 V. The energy conversion efficiency takes negligible values in conditions where the probability for electrons to cross the junction is too small. This is the case for photon energies $\hbar\Omega$ significantly smaller than the work function W. Different possibilities exist to increase the electronic currents: (i) increase the amplitude $V_{\rm osc}$ of the external potential, (ii) reduce the work function W of the metallic contacts, (iii) reduce the gap spacing D between the cathode and the anode, (iv) increase the temperature T of the device, (v) consider in addition to $V_{\rm osc}\cos(\Omega t)$ a static biasing $V_{\rm stat}$, (vi) consider metals with different work functions in order to induce a contact potential through the junction. When considering these different possibilities, one must

however preserve the capacity of the junction to rectify oscillating potentials. We will only consider the effects of changing $V_{\rm osc}$, W and D. The examination of other possibilities will be left for future work.

The mean diode current $< I >$ and the mean energy $< P_{\rm in,osc} >$ required per unit of time to establish the oscillating field both increase proportionally to $V_{\rm osc}^2$. The energy conversion efficiency $\eta_{\rm ECE}$, which is given by $\eta_{\rm ECE} = [< I >^2 /(dI_{\rm stat}/dV_{\rm stat})]/ < P_{\rm in,osc} >$ when $V_{\rm stat}$=0 V, will therefore increase proportionally to $V_{\rm osc}^2$ if the mean diode current $< I >$ is indeed unaffected by higher-order terms. The increase of $\eta_{\rm ECE}$ will actually be stronger in conditions where these higher-order terms must be considered. This is illustrated in Fig. 6, where we increased the amplitude $V_{\rm osc}$ of the oscillating potential from 0.1 V to 1 V. The energy conversion efficiencies achieved when using the classical expression $< I_{\rm CL} >$ or the finite-difference expression $< I_{\rm FD} >$ increase proportionally to $V_{\rm osc}^2$. The results obtained when using the Tien-Gordon expression $< I_{\rm TG} >$ or the time-dependent transfer-matrix results $< I_{\rm TM} >$ exhibit however a more significant increase. An energy conversion efficiency of 3.5×10^{-3} is achieved for a photon energy $\hbar\Omega$ of 2.5 eV in the middle of the visible spectrum.

The results obtained when the work function W of the metallic contacts is reduced to 1.5 eV are represented in Fig. 7 (a lowering of the work function can be achieved by coating the materials with cesium).[38,49] The results correspond to an amplitude $V_{\rm osc}$ for the oscillating voltage of respectively 0.1 V and 1 V. These results show that decreasing the work function W significantly enhances the energy conversion efficiency of the diode. An energy conversion efficiency of 2.5×10^{-3} is achieved for a photon energy $\hbar\Omega$ of 1.3 eV when considering an oscillating-voltage amplitude $V_{\rm osc}$ of 0.1 V. When increasing $V_{\rm osc}$ to 1 V, the mean diode current $< I >$ turns out to be significantly affected by higher-order terms (these terms are responsible for the deviations between the results achieved by using the finite-difference expression $< I_{\rm FD} >$ and those provided by the Tien-Gordon expression $< I_{\rm TG} >$). We reach in this case an energy conversion efficiency of 24% for the same photon energy $\hbar\Omega$ of 1.3 eV.

We can compare the results obtained so far for a gap spacing D of 2 nm with those achieved when reducing this gap spacing D to a value of 1.5 nm (spacing of 0.5 nm between the apex of the protrusion and the anode). We keep an amplitude $V_{\rm osc}$ of 1 V for the amplitude of the oscillating potential. The energy conversion efficiencies achieved by using the models of Sec. II and III for the calculation of $< I >$ are represented in Fig. 8. This figure presents the results obtained when considering a work function W of either 4.5 eV or

1.5 eV for the two metals.

Reducing the gap spacing D has two important effects. On one side, we reduce the width of the tunneling barrier. We also reduce the height of this barrier because of the larger effective field in the junction and because of the overlap between (multiple) image interactions between the electrons that cross the junction and the metallic elements in this junction. These two effects increase the probability that electrons have to cross the junction. This in turn reduces the impedance $R = 1/(dI_{\rm stat}/dV_{\rm stat})$ of the junction and therefore the RC-response time of the device (the increase of the capacitance C is far less influential on the RC-time constant than the reduction achieved for the impedance R).[5] On the other hand, reducing the gap spacing D will reduce the rectification capacity of the junction, which is however necessary to convert the energy of the oscillating field. For energy regions in which tunneling is required in order for electrons to cross the junction, the increase in the tunneling probability will be the dominant factor and higher energy conversion efficiencies will be achieved. For energy regions in which ballistic motion over the barrier is possible, the reduction in the rectification capacity of the junction will be the dominant factor and smaller energy conversion efficiencies will be obtained. This is the case with photon energies $\hbar\Omega$ that exceed the height of the surface barrier, as illustrated in Fig. 8 when considering a work function W of 1.5 eV. For the situation considered, reducing the gap spacing D to a value of 1.5 nm when considering a work function W of 1.5 eV has the effect to reduce the energy conversion efficiency $\eta_{\rm ECE}$. It has however the effect to reduce the RC-response time of the device from a value of 7×10^{-13} sec (value for D=2 nm) to a value of 6.5×10^{-15} sec (value for D=1.5 nm). This makes actually the junction biasing more efficient when considering optical frequencies.

VI. CONCLUSIONS

We used different models to analyze the efficiency with which the energy of external radiations can be converted using geometrically asymmetric metal-vacuum-metal junctions. The frequencies considered ranged from the infrared through the visible. The transfer-matrix methodology that enables the quantum-mechanical modeling of these junctions was improved. In its current form, it provides results that are fully consistent in the limit when $\hbar\Omega \rightarrow 0$ with those provided by semi-classical extrapolations of static current-voltage data.

When considering optical frequencies, the time taken by electrons to cross the junction becomes comparable with the period of the oscillating barrier. In addition, the absorption of energy quanta $\hbar\Omega$ increases significantly the probability that electrons have to cross the junction. Classical arguments fail in this context at providing a suitable description of the device and a quantum-mechanical modeling must be used instead. We analyzed parameters that determine the efficiency with which energy is converted in these junctions (we focussed in this work on the amplitude $V_{\rm osc}$ of the oscillating voltage, on the work function W of the metallic contacts, and on the gap spacing D between these contacts). In conditions where the mean diode current $< I >$ is merely proportional to $V_{\rm osc}^2$ (lowest-order approximation), the efficiency with which energy is converted by the device turns out to increase proportionally to $V_{\rm osc}^2$. A stronger increase was observed in conditions where the mean diode current $< I >$ is significantly affected by higher-order terms (this was the case when considering an oscillating-voltage amplitude $V_{\rm osc}$ of 1 V). The results indicate that the work function W of the metallic contacts should be as small as possible in order to increase the probability that electrons have to cross the junction. Reducing the gap spacing D will also increase this probability. This will reduce in turn the RC-response time of the device. Reducing the gap spacing D however reduces the rectification capacity of the junction so that an optimal balance between these different factors must be found. Other possibilities exist to increase the efficiency with which energy is converted in these junctions. Their examination will be left for future work.

Acknowledgments

A.M. is funded as Research Associate by the National Fund for Scientific Research (FNRS) of Belgium. This work used resources of the Interuniversity Scientific Computing Facility located at the University of Namur, Belgium, which is supported by the F.R.S.-FNRS under convention No. 2.4617.07. The authors acknowledge the support of the Paul H. Cutler Endowment Fund for Excellence of the Eberly College of Science, The Pennsylvania State University. O. Deparis is acknowledged for his interest in this problem and for stimulating discussions.

APPENDIX A: MEAN DIODE CURRENT $< I >$ AND MEAN ENERGY $< P >$ GAINED PER UNIT OF TIME BY THE ELECTRONS THAT CROSS THE JUNCTION

We derive here the expression 6 used to compute the mean energy $< P >$ gained per unit of time from the source of the external potential by the electrons that cross the junction. The expression 5 for the mean diode current $< I >$ will result naturally from this derivation. Let us consider for the moment a single scattering solution $\Psi^{+}_{m,j,0}$ (these solutions contribute to the upward current). $\Psi^{+}_{m,j,0}$ is given in Region III by

$$\Psi^{+}_{m,j,0} = \sum_{m',j',k'} S^{++}_{(m',j',k'),(m,j,0)} \Psi^{\mathrm{III},+}_{m',j',k'}, \tag{A1}$$

where the boundary states $\Psi^{\mathrm{III},+}_{m',j',k'}$ are given by

$$\Psi^{\mathrm{III},+}_{m',j',k'} = \Phi_{m',j'}(\rho,\phi) e^{i\sqrt{\frac{2m}{\hbar^2}(E+\lambda_{k'}-\hat{V}_{\mathrm{III}})-k^2_{m',j'}}z} \sum_{k''=-N}^{N} V_{k'',k'} e^{-i(E+k''\hbar\Omega)t/\hbar} \tag{A2}$$

with $\Phi_{m',j'}(\rho,\phi) = RJ_{m'}(k_{m',j'}\rho)\exp(im'\phi)/\sqrt{2\int_0^R \rho J^2_{m'}(k_{m',j'}\rho)d\rho}$ and $\hat{V}_{\mathrm{III}} = -W - E_{\mathrm{F}}$.[2] The functions $\Phi_{m',j'}(\rho,\phi)$ have the property that $\int_0^{2\pi} d\phi \int_0^R \rho \Phi^{*}_{m_1,j_1}(\rho,\phi)\Phi_{m_2,j_2}(\rho,\phi)d\rho = \pi R^2 \delta_{m_1,m_2}\delta_{j_1,j_2}$. $\lambda_{k'}$ and $V_{k'',k'}$ refer to the eigenvalues and the k''-components of the corresponding eigenvectors of a matrix M, whose elements are defined by $M_{k'',k'} = k'\hbar\Omega\delta_{k'',k'} + \frac{eV_{\mathrm{osc}}}{2}(\delta_{k'',k'+1} + \delta_{k'',k'-1})$.[2]

The z-component of the flux of total energy associated with $\Psi^{\mathrm{III},+}_{m,j,0}$ is given by $S^{+}_{z;m,j,0} = \frac{\hbar}{2mi}(H\Psi^{\mathrm{III},+\,*}_{m,j,0}\frac{d}{dz}\Psi^{\mathrm{III},+}_{m,j,0} - H\Psi^{\mathrm{III},+}_{m,j,0}\frac{d}{dz}\Psi^{\mathrm{III},+\,*}_{m,j,0})$, where $H = -\frac{\hbar^2}{2m}\Delta + \hat{V}_{\mathrm{III}} - eV_{\mathrm{osc}}(e^{i\Omega t} + e^{-i\Omega t})/2$ refers to the Hamiltonian in Region III (V_{osc} is the amplitude of the oscillating part of the electric potential). We can then calculate that

$$\begin{aligned} H\Psi^{\mathrm{III},+}_{m,j,0} &= \sum_{k',m',j'} S^{++}_{(m',j',k'),(m,j,0)} \Phi_{m',j'}(\rho,\phi) e^{i\sqrt{\frac{2m}{\hbar^2}(E+\lambda_{k'}-\hat{V}_{\mathrm{III}})-k^2_{m',j'}}z} e^{-iEt/\hbar} \\ &\times \left\{ (E+\lambda_{k'}) \sum_{k''} V_{k'',k'} e^{-ik''\Omega t} - \frac{eV_{\mathrm{osc}}}{2} \sum_{k''} V_{k'',k'} [e^{-i(k''-1)\Omega t} + e^{-i(k''+1)\Omega t}] \right\} \end{aligned} \tag{A3}$$

and

$$\begin{aligned} \frac{d}{dz}\Psi^{\mathrm{III},+}_{m,j,0} &= \sum_{k',m',j'} S^{++}_{(m',j',k'),(m,j,0)} \Phi_{m',j'}(\rho,\phi) i\sqrt{\frac{2m}{\hbar^2}(E+\lambda_{k'}-\hat{V}_{\mathrm{III}}) - k^2_{m',j'}} \\ &\times e^{i\sqrt{\frac{2m}{\hbar^2}(E+\lambda_{k'})-k^2_{m',j'}}z} e^{-iEt/\hbar} \sum_{k''} V_{k'',k'} e^{-ik''\Omega t}. \end{aligned} \tag{A4}$$

The time-averaged value for the flux of total energy achieved over the cylindrical surface spanned by ρ and ϕ is then given by

$$\begin{aligned} < S^{+}_{z;m,j,0} >_t \; &= \; \frac{\Omega}{2\pi}\int_0^{2\pi/\Omega} dt \int_0^{2\pi} d\phi \int_0^{R} \rho S^{+}_{z;m,j,0} d\rho \\ &= \; \frac{\hbar\pi R^2}{m}\mathrm{Re}\left\{ \sum_{m',j',k'_1,k'_2} \sqrt{\frac{2m}{\hbar^2}(E+\lambda_{k'_2}) - k^2_{m',j'}} \right. \\ &\times \; S^{++*}_{(m',j',k'_1),(m,j,0)} S^{++}_{(m',j',k'_2),(m,j,0)} e^{i\Delta k_{z;m',j',k'_1,k'_2} z} \\ &\times \; \left. \left[(E+\lambda_{k'_1}) \sum_{k''} V_{k'',k'_1} V_{k'',k'_2} - \frac{eV_{\mathrm{osc}}}{2} \sum_{k''} V_{k'',k'_1} (V_{k''-1,k'_2} + V_{k''+1,k'_2}) \right] \right\} \end{aligned} \tag{A5}$$

in which

$$\Delta k_{z;m',j',k'_1,k'_2} = \sqrt{\frac{2m}{\hbar^2}(E+\lambda_{k'_2} - \hat{V}_{\mathrm{III}}) - k^2_{m',j'}} - \sqrt{\frac{2m}{\hbar^2}(E+\lambda_{k'_1} - \hat{V}_{\mathrm{III}}) - k^2_{m',j'}}. \tag{A6}$$

From the equation that defines the eigenvalues $\lambda_{k'}$ and the components $V_{k'',k'}$ of the corresponding eigenvectors, one can show that $(E+\lambda_{k'_1})\sum_{k''} V_{k'',k'_1} V_{k'',k'_2} - \frac{eV_{\mathrm{osc}}}{2}\sum_{k''} V_{k'',k'_1}(V_{k''-1,k'_2} + V_{k''+1,k'_2}) = \sum_{k''}(E+k''\hbar\Omega) V_{k'',k'_1} V_{k'',k'_2}$. If we average $< S^{+}_{z;m,j,0} >_t$ over z in Region III, the factor $e^{i\Delta k_{z;m',j',k'_1,k'_2} z}$ will actually select the terms associated with $k'_1 = k'_2$. With N sufficiently large to get an accurate representation of the boundary states in Region III, we then have $\sum_{k''}(E+k''\hbar\Omega)|V_{k'',k'}|^2 = E + k'\hbar\Omega$.[2] The z-averaged value of $< S^{+}_{z;m,j,0} >_t$ can hence be written as

$$< S^{+}_{z;m,j,0} >_{z,t} \; = \; \frac{\hbar\pi R^2}{m} \sum_{m',j',k'} (E+k'\hbar\Omega) \sqrt{\frac{2m}{\hbar^2}(E+\lambda_{k'} - \hat{V}_{\mathrm{III}}) - k^2_{m',j'}} |S^{++}_{(m',j',k'),(m,j,0)}|^2 \tag{A7}$$

where the summations are restricted to propagative states. This result corresponds to a flux of total energy. A flux of kinetic energy is obtained by substracting in Eq. A7 the constant part $\hat{V}_{\mathrm{III}}$ of the potential energy in Region III, hence giving

$$< P^{+}_{m,j,0} > \; = \; \frac{\hbar\pi R^2}{m} \sum_{m',j',k'} (E+k'\hbar\Omega - \hat{V}_{\mathrm{III}}) \sqrt{\frac{2m}{\hbar^2}(E+\lambda_{k'} - \hat{V}_{\mathrm{III}}) - k^2_{m',j'}} |S^{++}_{(m',j',k'),(m,j,0)}|^2 \tag{A8}$$

as contribution of the scattering solution $\Psi^{+}_{m,j,0}$ to the z and t-averaged flux of kinetic energy in Region III.

The density of states $\mathcal{D}_{m,j,0}(E)$ associated with the solution $\Psi^{+}_{m,j,0}$ is given by

$$\mathcal{D}_{m,j,0}(E) = \frac{m}{\pi^2\hbar^2 R^2} \frac{1}{\sqrt{\frac{2m}{\hbar^2}(E - \hat{V}_{\mathrm{I}}) - k^2_{m,j}}}, \tag{A9}$$

with $\hat{V}_{\rm I} = eV_{\rm stat} - W - E_{\rm F}$.[2,43] The solution $\Psi^{+}_{m,j,0}$ is also associated with a Fermi factor $f_{\rm I}(E) = 1/\{1 + \exp[(E-\mu_{\rm I})/(k_{\rm B}T)]\}$ in which $\mu_{\rm I} = eV_{\rm stat} - W$. If we substract from $< P^{+}_{m,j,0} >$ the flux of kinetic energy $E - \hat{V}_{\rm I} = E - (\hat{V}_{\rm III} + eV_{\rm stat})$ in the region of incidence and integrate over every incoming state in Region I, we find that the mean value of the kinetic energy gained per unit of time by the electrons that contribute to the upward current is given by

$$< P^{+} >= \frac{2e}{h}\int_{\hat{V}_{\rm I}}^{+\infty} f_{\rm I}(E)\sum_{m,j}\sum_{k',m',j'}(V_{\rm stat} + k'\frac{\hbar\Omega}{e})\frac{v_{{\rm III},(m',j',k')}}{v_{{\rm I},(m,j,0)}}|S^{++}_{(m',j',k'),(m,j,0)}|^2 dE, \quad \text{(A10)}$$

where we define the group velocities in Region I and III by $v_{{\rm I},(m,j,k)} = \frac{\hbar}{m}\sqrt{\frac{2m}{\hbar^2}(E + k\hbar\Omega - \hat{V}_{\rm I}) - k^2_{m,j}}$ and $v_{{\rm III},(m,j,k)} = \frac{\hbar}{m}\sqrt{\frac{2m}{\hbar^2}(E + \lambda_k - \hat{V}_{\rm III}) - k^2_{m,j}}$. The mean upward current associated with these electrons is finally given by

$$< I^{+} >= \frac{2e}{h}\int_{\hat{V}_{\rm I}}^{+\infty} f_{\rm I}(E)\sum_{m,j}\sum_{k',m',j'}\frac{v_{{\rm III},(m',j',k')}}{v_{{\rm I},(m,j,0)}}|S^{++}_{(m',j',k'),(m,j,0)}|^2 dE. \quad \text{(A11)}$$

We can analyze in a similar way the kinetic energy gained per unit of time by the electrons that contribute to the downward current. The mean value achieved for this quantity will be given by

$$< P^{-} >= \frac{2e}{h}\int_{\hat{V}_{\rm III}}^{+\infty} f_{\rm III}(E)\sum_{m,j}\sum_{k',m',j'}(-V_{\rm stat} + k'\frac{\hbar\Omega}{e})\frac{v_{{\rm I},(m',j',k')}}{v_{{\rm III},(m,j,0)}}|S^{--}_{(m',j',k'),(m,j,0)}|^2 dE, \quad \text{(A12)}$$

with a corresponding mean downward current $< I^{-} >$ given by

$$< I^{-} >= \frac{2e}{h}\int_{\hat{V}_{\rm III}}^{+\infty} f_{\rm III}(E)\sum_{m,j}\sum_{k',m',j'}\frac{v_{{\rm I},(m',j',k')}}{v_{{\rm III},(m,j,0)}}|S^{--}_{(m',j',k'),(m,j,0)}|^2 dE. \quad \text{(A13)}$$

Adding Eq. A10 with Eq. A12 will provide Eq. 6 for the mean energy $< P >$ gained per unit of time from the source of the external potential by the electrons that cross the junction, while adding Eq. A11 with Eq. A13 will provide Eq. 5 for the mean diode current $< I >$. Since we define $< P >$ as the energy gained per unit of time *from the source of the external potential*, it refers necessarily to the *kinetic energy* gained by these electrons. We consider in the text these specifications as implicitly understood.

APPENDIX B: THE USE OF $f(E)$ AND $[1 - f(E)]$ FERMI FACTORS IN THE TRANSFER-MATRIX METHODOLOGY

The mean diode current $< I >$ in a metal-vacuum-metal junction that is subject to a potential $V(t) = V_{\rm stat} + V_{\rm osc}\cos(\Omega t)$ can be calculated using Eq. 5 in Sec. II. When the

junction is only subject to a *static potential*, this mean diode current is actually given by

$$< I > = \frac{2e}{h}\int_{\hat{V}_{\rm I}}^{+\infty} f_{\rm I}(E)\sum_{m,j}\sum_{m',j'}\frac{\sqrt{\frac{2m}{\hbar^2}(E-\hat{V}_{\rm III})-k_{m',j'}^2}}{\sqrt{\frac{2m}{\hbar^2}(E-\hat{V}_{\rm I})-k_{m,j}^2}}|S^{++}_{(m',j'),(m,j)}|^2dE$$
$$- \frac{2e}{h}\int_{\hat{V}_{\rm III}}^{+\infty} f_{\rm III}(E)\sum_{m,j}\sum_{m',j'}\frac{\sqrt{\frac{2m}{\hbar^2}(E-\hat{V}_{\rm I})-k_{m',j'}^2}}{\sqrt{\frac{2m}{\hbar^2}(E-\hat{V}_{\rm III})-k_{m,j}^2}}|S^{--}_{(m',j'),(m,j)}|^2dE, \qquad \text{(B1)}$$

where $\hat{V}_{\rm I} = eV_{\rm stat} - W - E_{\rm F}$ and $\hat{V}_{\rm III} = -W - E_{\rm F}$. There is in this case no coupling between states associated with different values of the energy and the summations are thus limited to the subscripts m and j that enumerate the lateral wavevectors $k_{m,j}$ (these summations are restricted to propagative states). The Fermi factors $f_{\rm I}(E) = 1/\{1+\exp[(E-\mu_{\rm I})/(k_{\rm B}T)]\}$ and $f_{\rm III}(E) = 1/\{1+\exp[(E-\mu_{\rm III})/(k_{\rm B}T)]\}$, in which $\mu_{\rm I} = eV_{\rm stat} - W$ and $\mu_{\rm III} = -W$, account for the filling of the electronic states in the regions that provide the electrons (i.e., Region I for the upward current and Region III for the downward current). The upward and downward currents will partially cancel each other, to a degree that reflects implicitly the availability of states in the region of transmission (i.e., Region III for the upward current and Region I for the downward current).

We can artificially substract from the first line of Eq. B1 the expression

$$\int_{\min(\hat{V}_{\rm I},\hat{V}_{\rm III})}^{+\infty} f_{\rm I}(E)f_{\rm III}(E)\sum_{m,j}\sum_{m',j'}\frac{\sqrt{\frac{2m}{\hbar^2}(E-\hat{V}_{\rm III})-k_{m',j'}^2}}{\sqrt{\frac{2m}{\hbar^2}(E-\hat{V}_{\rm I})-k_{m,j}^2}}|S^{++}_{(m',j'),(m,j)}|^2dE$$

if we add the same expression to the second line of Eq. B1. Provided the relation

$$\sum_{m,j}\sum_{m',j'}\frac{\sqrt{\frac{2m}{\hbar^2}(E-\hat{V}_{\rm III})-k_{m',j'}^2}}{\sqrt{\frac{2m}{\hbar^2}(E-\hat{V}_{\rm I})-k_{m,j}^2}}|S^{++}_{(m',j'),(m,j)}|^2 = \sum_{m,j}\sum_{m',j'}\frac{\sqrt{\frac{2m}{\hbar^2}(E-\hat{V}_{\rm I})-k_{m',j'}^2}}{\sqrt{\frac{2m}{\hbar^2}(E-\hat{V}_{\rm III})-k_{m,j}^2}}|S^{--}_{(m',j'),(m,j)}|^2 \qquad \text{(B2)}$$

holds for any value of the energy E, the mean diode current $< I >$ can actually be written as

$$< I > = \frac{2e}{h}\int_{\hat{V}_{\rm I}}^{+\infty} f_{\rm I}(E)[1-f_{\rm III}(E)]\sum_{m,j}\sum_{m',j'}\frac{\sqrt{\frac{2m}{\hbar^2}(E-\hat{V}_{\rm III})-k_{m',j'}^2}}{\sqrt{\frac{2m}{\hbar^2}(E-\hat{V}_{\rm I})-k_{m,j}^2}}|S^{++}_{(m',j'),(m,j)}|^2dE$$
$$- \frac{2e}{h}\int_{\hat{V}_{\rm III}}^{+\infty} f_{\rm III}(E)[1-f_{\rm I}(E)]\sum_{m,j}\sum_{m',j'}\frac{\sqrt{\frac{2m}{\hbar^2}(E-\hat{V}_{\rm I})-k_{m',j'}^2}}{\sqrt{\frac{2m}{\hbar^2}(E-\hat{V}_{\rm III})-k_{m,j}^2}}|S^{--}_{(m',j'),(m,j)}|^2dE, \qquad \text{(B3)}$$

which is therefore equivalent to Eq. B1 *in the case of a static barrier*. This is the formulation used in our previous work.[1]

The relation B2 is a consequence of the reciprocity of the **S**-matrix.[50] Numerical calculations achieved using either Eq. B1 or Eq. B3 turn out indeed to be identical when considering a static barrier. The factors $[1 - f_{\rm III}(E)]$ and $[1 - f_{\rm I}(E)]$ account explicitly for the availability of free states in the regions of transmission. Eq. B3 has the advantage over Eq. B1 to offer a faster convergence when considering the upward and downward currents separately. The factors $f_{\rm I}(E)[1 - f_{\rm III}(E)]$ and $f_{\rm III}(E)[1 - f_{\rm I}(E)]$ define indeed an energy window that limits the integration over E. These factors $[1 - f_{\rm III}(E)]$ and $[1 - f_{\rm I}(E)]$ are however not appropriate in the case of an oscillating barrier.

When considering an oscillating barrier, one must compute the mean diode current $< I >$ by using Eq. 5. A transformation of Eq. 5 to a form similar to Eq. B3 is not valid in the case of an oscillating barrier. The reason comes from the fact

$$\sum_{m,j}\sum_{k',m',j'} \frac{\sqrt{\frac{2m}{\hbar^2}(E+\lambda_{k'}-\hat{V}_{\rm III})-k^2_{m',j'}}}{\sqrt{\frac{2m}{\hbar^2}(E-\hat{V}_{\rm I})-k^2_{m,j}}} |S^{++}_{(m',j',k'),(m,j,0)}|^2$$
$$\neq \sum_{m,j}\sum_{k',m',j'} \frac{\sqrt{\frac{2m}{\hbar^2}(E+k'\hbar\Omega-\hat{V}_{\rm I})-k^2_{m',j'}}}{\sqrt{\frac{2m}{\hbar^2}(E-\hat{V}_{\rm III})-k^2_{m,j}}} |S^{--}_{(m',j',k'),(m,j,0)}|^2 \qquad \text{(B4)}$$

when considering the scattering solutions achieved in the case of an oscillating barrier. Unlike Eq. B2, the summations in Eq. B4 do not include the whole set of propagative states in Region I and III and the reciprocity of the **S**-matrix can not be used. The discrepancy between the results achieved when computing the mean diode current $< I >$ by Eq. 5 or by an expression that includes factors of the form $[1 - f_{\rm III}(E)]$ and $[1 - f_{\rm I}(E)]$ was illustrated in Fig. 2. A similar discrepancy in the results achieved when computing the mean energy $< P >$ gained per unit of time from the source of the external potential by the electrons that cross the junction was illustrated in Fig. 3.

---

[1] A. Mayer, M.S. Chung, B.L. Weiss, N.M. Miskovsky, and P.H. Cutler, Phys. Rev. B **77**, 085411 (2008).

[2] A. Mayer, M.S. Chung, B.L. Weiss, N.M. Miskovsky, and P.H. Cutler, Phys. Rev. B **78**, 205404 (2008).

[3] A. Mayer and P.H. Cutler, J. Phys. Condens. Mat. **21**, 395304 (2009).

[4] A. Mayer, M.S. Chung, B.L. Weiss, N.M. Miskovsky, and P.H. Cutler, Nanotechnology **21**, 145204 (2010).

[5] A. Mayer, M.S. Chung, P.B. Lerner, B.L. Weiss, N.M. Miskovsky, and P.H. Cutler, J. Vac. Sci. Technology B **29**, 041802 (2011).

[6] T.E. Sullivan, P.H. Cutler, and A.A. Lucas, Surf. Science **54**, 561 (1976).

[7] K.M. Evenson, G.W. Day, J.S. Wells, and L.O. Mullen, Appl. Phys. Lett. **20**, 133 (1972).

[8] W. Krieger, T. Suzuki, M. Volcker, and H. Walther, Phys. Rev. B **41**, 10229 (1990).

[9] N.M. Miskovsky, S.H. Park, P.H. Cutler, and T.E. Sullivan, J. Vac. Sci. Technol. B **12**, 2148 (1994).

[10] C. Fumeaux, W. Herrmann, F.K. Kneubuhl, and H. Rothuizen, Infrared Phys. Technol. **39**, 123 (1998).

[11] N. Beverini, G. Carelli, E. Ciaramella, G. Contestabile, A. De Michele, and M. Presi, Laser Physics **15**, 1334 (2005).

[12] L.O. Hocker, D.R. Sokoloff, V. Daneu, A. Szoke, and A. Javan, Appl. Phys. Lett. **12**, 401 (1968).

[13] J.F. Mulligan, Amer. J. Phys. **44**, 960 (1976).

[14] J. Terrien, Rep. Prog. Phys. **39**, 1067 (1976).

[15] K.M. Evenson, J.S. Wells, F.R. Peterson, B.L. Danielson, G.W. Day, R.L. Barger, and J.L. Hall, Phys. Rev. Lett. **29**, 1346 (1972).

[16] *Proceedings of the 17th General Conference on Measures and Weights*, Sevres, France (Comptes Rendus, BIPM, 1983), p. 93.

[17] T.E. Sullivan, Y. Kuk, and P.H. Cutler, IEEE Trans. Electron Devices **36**, 2659 (1989).

[18] A.A. Lucas, P.H. Cutler, T.E. Feuchtwang, T.T. Tsong, T.E. Sullivan, Y. Yuk, H. Nguyen, and P.J. Silverman, J. Vac. Sci. Technol. A **6**, 461 (1988).

[19] H.Q. Nguyen, P.H. Cutler, T.E. Feuchtwang, Z.-H. Huang, Y. Kuk, P.J. Silverman, A.A. Lucas, and T.E. Sullivan, IEEE Trans. Electron Devices **36**, 2671 (1989).

[20] A.A. Lucas, A. Moussiaux, M. Schmeits, and P.H. Cutler, Communication on Physics **2**, 169-74 (1977).

[21] N.M. Miskovsky, S.J. Shepherd, P.H. Cutler, T.E. Sullivan, and A.A. Lucas, Appl. Phys. Lett. **35**, 560 (1979)

[22] T.E. Sullivan, P.H. Cutler, and A.A. Lucas, Surf. Science **62**, 455 (1977).

[23] K.B. Crozier, A. Sundaramurthy, G.S. Kino, and C.F. Quate, J. Appl. Phys. **94**, 4632 (2003).

[24] T.-D. Onuta, M. Waegele, C.C. DuFort, W.L. Schaich, and B. Dragnea, Nano Letters **7**, 557 (2007).

[25] D.K. Kotter, S.D. Novack, W.D. Slafer, and P.J. Pinhero, J. Sol. Energy Eng. **132**, 011014 (2010).

[26] K. Choi, F. Yesilkoy, G. Ryu, S.H. Cho, N. Goldsman, M. Dagenais, and M. Peckerar, IEEE Trans. Electron Devices **58**, 3519 (2011).

[27] J.A. Bean, A. Weeks, and G.D. Boreman, IEEE J. Quantum Electronics **47**, 126 (2011).

[28] T.E. Hartman, J. Appl. Phys. **33**, 3427 (1962).

[29] Z.H. Huang, P.H. Cutler, T.E. Feuchtwang, E. Kazes, H.Q. Nguyen, and T.E. Sullivan, J. Vac. Sci. Technol. A **8**, 186 (1990).

[30] A.V. Bragas, S.M. Landi, and O.E. Martinez, Appl. Phys. Lett. **72**, 2075 (1998).

[31] P. Esfandiari, G. Bernstein, P. Fay, W. Porod, B. Rakos, A. Zarandy, B. Berland, L. Boloni, G. Boreman, B. Lail, B. Monacelli, and A. Weeks, Proc. of the SPIE **5783**, 470 (2005).

[32] P.C.D. Hobbs, R.B. Laibowitz, F.R. Libsch, N.C. LaBianca, and P.P. Chiniwalla, Optics Express **15**, 16376 (2007).

[33] M. Dagenais, K. Choi, F. Yesilkoy, A.N. Chryssis, and M.C. Peckerar, Proc. of SPIE **7605**, 76050E-1 (2010).

[34] D.R. Ward, F. Huser, F. Pauly, J.C. Cuevas, and D. Natelson, Nature Nanotechnology **5**, 732 (2010).

[35] F. Yesilkoy, K. Choi, M. Dagenais, and M. Peckerar, Solid State Electron. **54**, 1211 (2010).

[36] K. Choi, F. Yesilkoy, A. Chryssis, M. Dagenais, and M. Peckerar, IEEE Electr. Device L. **31**, 809 (2010).

[37] M. Tonouchi, Nature Photonics **1**, 97 (2007).

[38] J.W. Schwede, I. Bargatin, D.C. Riley, B.E. Hardin, S.J. Rosenthal, Y. Sun, F. Schmitt, P. Pianetta, R.T. Howe, Z.-X. Shen, and N.A. Melosh, Nature Materials **9**, 762 (2010).

[39] A. Mayer and Ph. Lambin, Nanotechnology **16**, 2685 (2005).

[40] Th. Laloyaux, I. Derycke, J.-P. Vigneron, Ph. Lambin, and A.A. Lucas, Phys. Rev. B **47**, 7508 (1993).

[41] F.H.M. Faisal, *Theory of Multiphoton Processes* (Plenum, New York, 1987), pp. 8-10.

[42] A. Pimpale, S. Holloday, and R.J. Smith, J. Phys. A **24**, 3533 (1991).

[43] A. Mayer and J.-P. Vigneron, Phys. Rev. B **56**, 12599 (1997).

[44] A. Mayer and J.-P. Vigneron, Ultramicroscopy **79**, 35 (1999).

[45] J.R. Tucker, IEEE J. Quant. Electron. **QE-15**, 1234 (1979).

[46] R.W. van der Heijden, J.H.M. Stoelinga, H.M. Swartjes, and P. Wyder, Solid State Commun. **39**, 133 (1981).

[47] P.K. Tien and J.P. Gordon, Phys. Rev. **129**, 647 (1963).

[48] R. Gupta and B.G. Willis, Appl. Phys. Lett. **90**, 253102 (2007).

[49] V.S. Fomenko, *Handbook of Thermionic Properties* (Plenum, New York, 1966), p. 20.

[50] M. Buttiker, IBM J. Res. Develop. **32**, 317 (1988).

FIGURE CAPTIONS

FIG. 1. Static part $\hat{V}_{\rm stat}(\mathbf{r})$ (left) and oscillating part $\hat{V}_{\rm osc}(\mathbf{r}) = \hat{V}_{\rm osc}(\mathbf{r},\Omega) = \hat{V}_{\rm osc}(\mathbf{r},-\Omega)$ (right) of the potential energy $\hat{V}(\mathbf{r},t) = \hat{V}_{\rm stat}(\mathbf{r}) + \hat{V}_{\rm osc}(\mathbf{r})\cos(\Omega t)$ that is used for the time-dependent transfer-matrix simulations. The gap spacing D is 2 nm. The radius of the hemispherical protrusion is 1 nm. The junction is subject to an electric potential $V(t) = V_{\rm stat} + V_{\rm osc}\cos(\Omega t)$, where $V_{\rm stat}$=0 V and $V_{\rm osc}$=0.1 V.

FIG. 2. Mean diode current $< I >$ provided by the classical expression $< I_{\rm CL} >$ (solid), the finite-difference expression $< I_{\rm FD} >$ (dashed), the Tien-Gordon expression $< I_{\rm TG} >$ (dot-dashed) and the time-dependent transfer-matrix technique $< I_{\rm TM} >$ (triangles). The representation also includes the results achieved using the transfer-matrix technique of Ref.[2] (cross). The gap spacing D is 2 nm. The static voltage $V_{\rm stat}$ is 0 V. The amplitude $V_{\rm osc}$ of the oscillating voltage is 0.1 V. The work function W is 4.5 eV. The temperature T is 300 K.

FIG. 3. Mean energy $< P >$ gained per unit of time by the electrons that cross the junction, as provided by the classical expression $< P_{\rm CL} >$ (solid), the finite-difference expression $< P_{\rm FD} >$ (dashed), the Tien-Gordon expression $< P_{\rm TG} >$ (dot-dashed) and the time-dependent transfer-matrix technique $< P_{\rm TM} >$ (triangles). The representation also includes the results achieved using the transfer-matrix technique of Ref.[2] (cross) as well as the result $< P_{\rm TM-CL} >$ achieved from a classical integration of the transfer-matrix currents (squares). The gap spacing D is 2 nm. The static voltage $V_{\rm stat}$ is 0 V. The amplitude $V_{\rm osc}$ of the oscillating voltage is 0.1 V. The work function W is 4.5 eV. The temperature T is 300 K.

FIG. 4. Quantum efficiency $\eta = \frac{[<I>-I_{\rm stat}]/[<P>-V_{\rm stat}I_{\rm stat}]}{e/\hbar\Omega}$ obtained when calculating $< I >$ and $< P >$ by the classical expressions $< I_{\rm CL} >$ and $< P_{\rm CL} >$ (solid), the finite-difference expressions $< I_{\rm FD} >$ and $< P_{\rm FD} >$ (dashed), the Tien-Gordon expressions $< I_{\rm TG} >$ and $< P_{\rm TG} >$ (dot-dashed) and the time-dependent transfer-matrix technique (triangles). The gap spacing D is 2 nm. The static voltage $V_{\rm stat}$ is 0 V. The amplitude $V_{\rm osc}$ of the oscillating voltage is 0.1 V. The work function W is 4.5 eV. The temperature T is 300 K.

FIG. 5. Energy conversion efficiency $\eta_{\rm ECE} = \frac{[<P_{\rm out,dc}> - V_{\rm stat} I_{\rm stat}]}{<P_{\rm in,osc}>}$ obtained when calculating $< I >$ by the classical expression $< I_{\rm CL} >$ (solid), the finite-difference expression $< I_{\rm FD} >$ (dashed), the Tien-Gordon expression $< I_{\rm TG} >$ (dot-dashed) and the time-dependent transfer-matrix technique (triangles). The gap spacing D is 2 nm. The static voltage $V_{\rm stat}$ is 0 V. The amplitude $V_{\rm osc}$ of the oscillating voltage is 0.1 V. The work function W is 4.5 eV. The temperature T is 300 K.

FIG. 6. Energy conversion efficiency $\eta_{\rm ECE} = \frac{[<P_{\rm out,dc}> - V_{\rm stat} I_{\rm stat}]}{<P_{\rm in,osc}>}$ obtained when calculating $< I >$ by the classical expression $< I_{\rm CL} >$ (solid), the finite-difference expression $< I_{\rm FD} >$ (dashed), the Tien-Gordon expression $< I_{\rm TG} >$ (dot-dashed) and the time-dependent transfer-matrix technique (triangles). The gap spacing D is 2 nm. The static voltage $V_{\rm stat}$ is 0 V. The amplitude $V_{\rm osc}$ of the oscillating voltage is 1 V. The work function W is 4.5 eV. The temperature T is 300 K.

FIG. 7. Energy conversion efficiency $\eta_{\rm ECE} = \frac{[<P_{\rm out,dc}> - V_{\rm stat} I_{\rm stat}]}{<P_{\rm in,osc}>}$ obtained when calculating $< I >$ by the classical expression $< I_{\rm CL} >$ (solid), the finite-difference expression $< I_{\rm FD} >$ (dashed), the Tien-Gordon expression $< I_{\rm TG} >$ (dot-dashed) and the time-dependent transfer-matrix technique (triangles). The gap spacing D is 2 nm. The static voltage $V_{\rm stat}$ is 0 V. The amplitude $V_{\rm osc}$ of the oscillating voltage is 0.1 V (left) and 1 V (right). The work function W is 1.5 eV. The temperature T is 300 K.

FIG. 8. Energy conversion efficiency $\eta_{\rm ECE} = \frac{[<P_{\rm out,dc}> - V_{\rm stat} I_{\rm stat}]}{<P_{\rm in,osc}>}$ obtained when calculating $< I >$ by the classical expression $< I_{\rm CL} >$ (solid), the finite-difference expression $< I_{\rm FD} >$ (dashed), the Tien-Gordon expression $< I_{\rm TG} >$ (dot-dashed) and the time-dependent transfer-matrix technique (triangles). The gap spacing D is 1.5 nm. The static voltage $V_{\rm stat}$ is 0 V. The amplitude $V_{\rm osc}$ of the oscillating voltage is 1 V. The work function W is 4.5 eV (left) and 1.5 eV (right). The temperature T is 300 K.

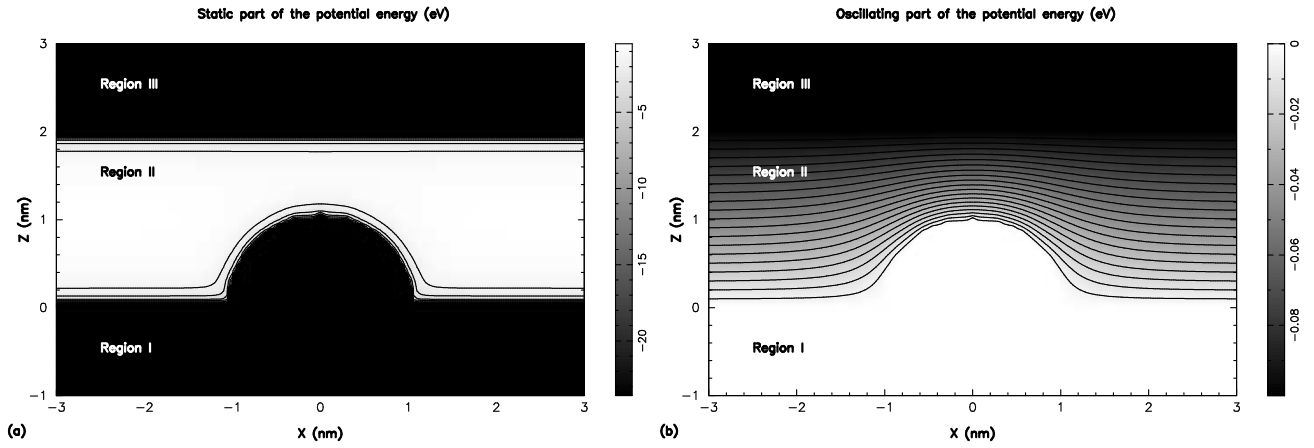
Static part of the potential energy (eV)
Region III
Region II
Region I
Z (nm)
X (nm)
(a)
Oscillating part of the potential energy (eV)
Region III
Region II
Region I
Z (nm)
X (nm)
(b)

FIG. 1

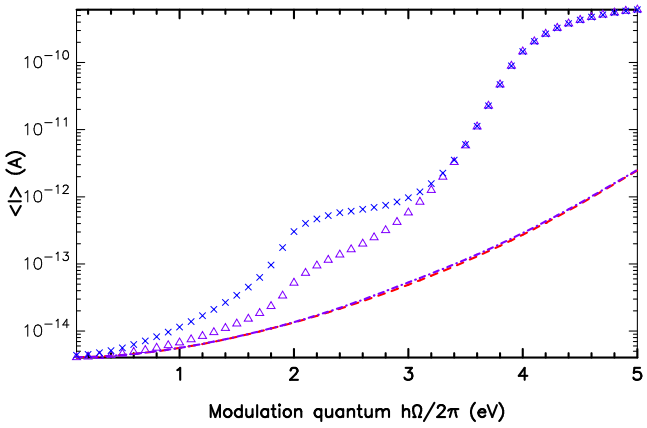
10^{-10}
10^{-11}
10^{-12}
10^{-13}
10^{-14}
<I> (A)
1
2
3
4
5
Modulation quantum hΩ/2π (eV)

FIG. 2

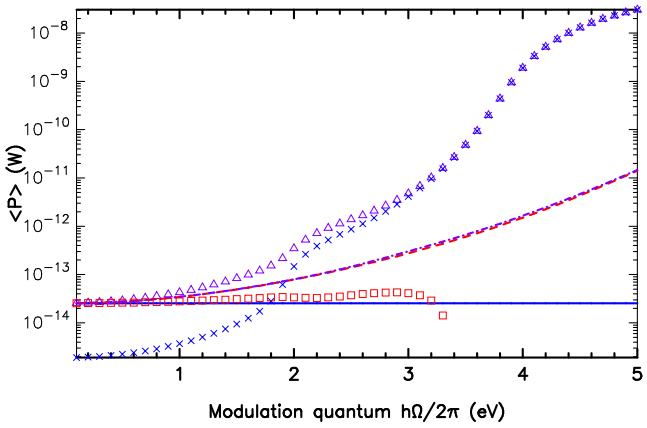
10^{-8}
10^{-9}
10^{-10}
10^{-11}
10^{-12}
10^{-13}
10^{-14}
<P> (W)
1
2
3
4
5
Modulation quantum hΩ/2π (eV)

FIG. 3

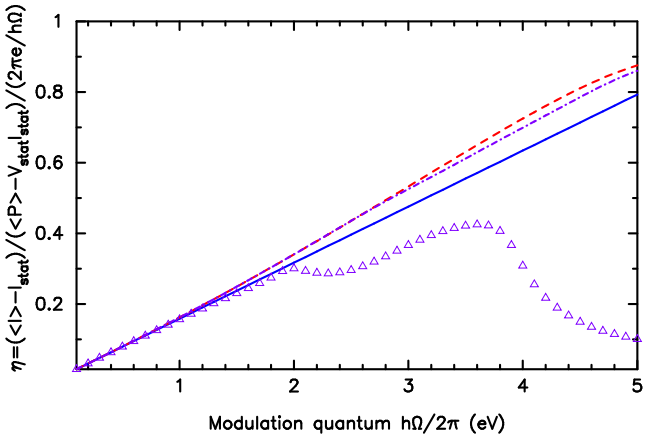
η=(<I>−I_stat)/(<P>−V_stat I_stat)/(2πe/hΩ)
1
0.8
0.6
0.4
0.2
1
2
3
4
5
Modulation quantum hΩ/2π (eV)

FIG. 4

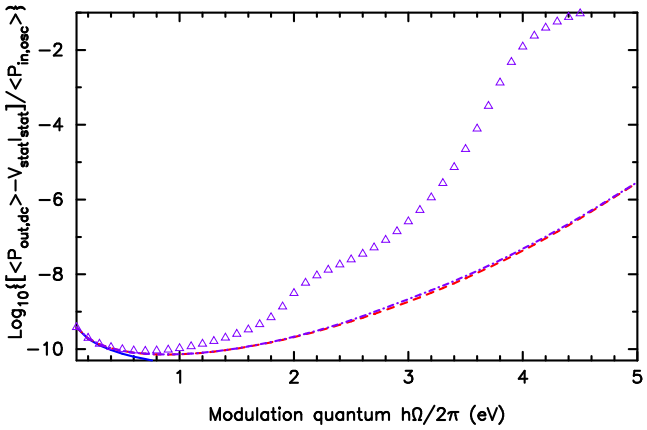
Log10{[<Pout,dc>−Vstat,stat'|stat>]/<Pin,osc>}
−2
−4
−6
−8
−10
1
2
3
4
5
Modulation quantum hΩ/2π (eV)

FIG. 5

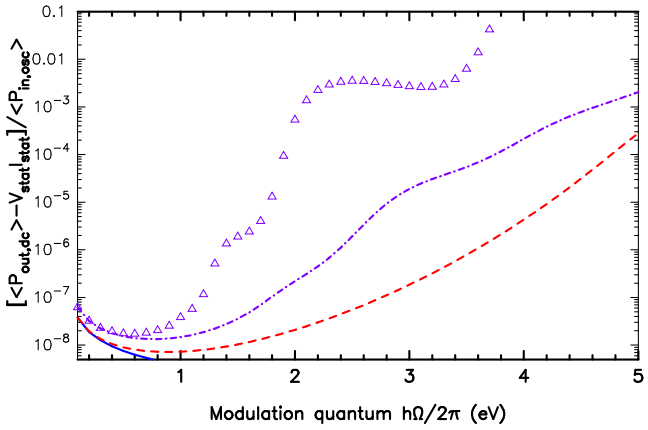
0.1
0.01
10^{-3}
10^{-4}
10^{-5}
10^{-6}
10^{-7}
10^{-8}
1
2
3
4
5
$[<P_{out,dc}>-V_{stat}I_{stat}]/<P_{in,osc}>$
Modulation quantum hΩ/2π (eV)

FIG. 6

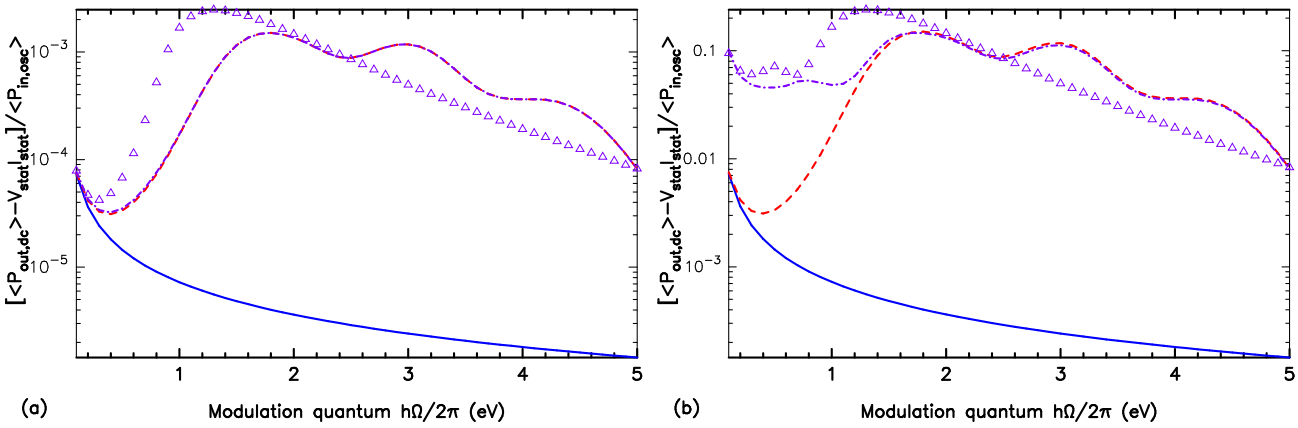
[<P_out,dc>−V_stat|_stat]/<P_in,osc>
10^−3
10^−4
10^−5
1
2
3
4
5
(a)
Modulation quantum hΩ/2π (eV)
0.1
0.01
10^−3
(b)

FIG. 7

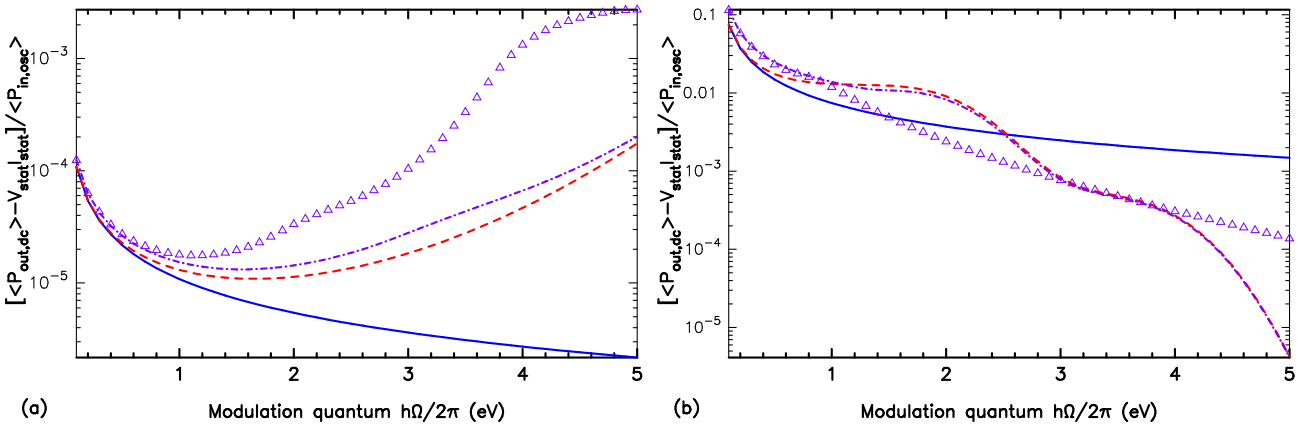
[<P_out,dc>−V_stat|stat|]/<P_in,osc>
10^−3
10^−4
10^−5
1
2
3
4
5
(a)
Modulation quantum hΩ/2π (eV)
0.1
0.01
10^−3
10^−4
10^−5
(b)
Modulation quantum hΩ/2π (eV)

FIG. 8